Porous Aromatic Frameworks

DOI: 10.1002/ange.201201381

Lithiated Porous Aromatic Frameworks with Exceptional Gas Storage Capacity**

Kristina Konstas, James W. Taylor, Aaron W. Thornton, Cara M. Doherty, Wei Xian Lim, Timothy J. Bastow, Danielle F. Kennedy, Colin D. Wood, Barry J. Cox, James M. Hill, Anita J. Hill, and Matthew R. Hill**

Gas storage has risen to prominence in recent years owing to the pressing need for solutions to mobile storage of alternative fuels, such as hydrogen[1,2] or methane,[3–5] and the environmental importance of capturing carbon dioxide.[6,7] The use of adsorbents has opened the possibility of high volumetric and gravimetric capacities at low operating pressures for these applications. In particular, the development of metal–organic frameworks (MOFs)[8] has been especially significant, given their high surface areas and periodic porosity, which satisfy the stipulated performance criteria[9] for widespread application of these materials.[3,10,11] However, many MOFs have low physiochemical stability,[12] and others are limited in their gravimetric capacities by the presence of heavy metal ions.[1]

Microporous organic polymers[13] are attractive in offsetting some of these issues, and a number of different classes of networks have been reported, including covalent organic frameworks (COFs)[14] and those based on C–C, C–H, and C–N bonds.[15] COFs have achieved some of the highest surface areas among the organic networks but also have limited physicochemical stability. Many of the other organic networks typically displayed lower surface areas until recently, when Ben et al. developed materials with surface areas in excess of those previously reported (Langmuir surface area of 7100 $m^2 g^{-1}$).[16] Porous aromatic frameworks (PAFs)[16–18] have shown exceptional surface areas, resulting in gas adsorption capacities as high as 158 $mg g^{-1}$ (H_2, 77 K, 90 bar), 389 $mg g^{-1}$ (CH_4, 295 K, 55 bar), and 2121 $mg g^{-1}$ (CO_2, 295 K, 50 bar).[18] Furthermore, these aromatic networks possess outstanding thermal and hydrothermal stability; however, they interact weakly with gases, which limits both the operating temperature the and overall gas storage capacity.[19] Previously reported methods for increasing adsorption enthalpy have included metalation,[13a,20] interpenetration,[21] optimization of pore size,[5,22] and pore infiltration with reactive species.[23]

Herein we present a route for the lithiation of PAF-1 (Li@PAF-1) that results in a reduced and consequently activated PAF surface (Scheme 1), delivering a low-pressure gas storage capacity increase of 22, 71, or 320 % for H_2, CH_4, and CO_2 respectively, compared to the native PAF-1. This increased capacity is due to enhanced adsorption enthalpies of up to 3.5 $kJ mol^{-1}$ in the case of H_2 storage, with enhancement continuing at high loadings owing to the delocalized charged surface. Here we have developed a synthetic method previously applied to conjugated microporous polymers (CMP)[13a] for attaining the challenging lithiated PAF-1 system (see the Supporting Information). We have comprehensively confirmed the reduction of the framework with solid-state ^1H, ^{13}C, ^6Li, and ^7Li MAS NMR spectroscopy, and the successful pore infiltration with complementary gas adsorption micropore analyses and positron annihilation lifetime spectroscopy (PALS). Mathematical predictions using the TIMTAM model[11] indicate the optimal pore structure and Li loading content of the lithiated PAF structures.

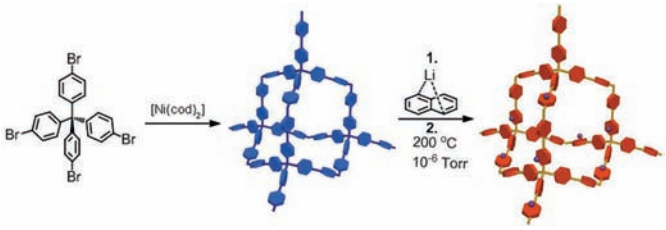

Scheme 1. Synthetic route to Li-PAF-1. Lithiation of PAF-1 (blue structure) reduces the framework at the π groups, activating it for gas storage.

Pore-size distribution analyses confirm that lithium ions have been successfully incorporated within the pores of PAF-1. DFT calculations based on Ar adsorption isotherms (Figure 1) show a clear shrinkage in pores owing to the incorporation of lithium ions and not of naphthalene, with pore-size maxima shrinking from 14 Å in PAF-1 to 11 Å in 5 %_Li@PAF-1. This pore filling is further confirmed with the PALS technique and atomistic simulation predictions (see the Supporting Information).

Solid-state NMR analyses indicate that PAF-1 is reduced by interaction with Li ions,[20] which are consequently bound

[*] Dr. K. Konstas, J. W. Taylor, Dr. A. W. Thornton, Dr. C. M. Doherty, W. X. Lim, Dr. T. J. Bastow, Dr. D. F. Kennedy, Dr. C. D. Wood, Dr. A. J. Hill, Dr. M. R. Hill
CSIRO Division of Materials Science and Engineering
Private Bag 33, Clayton South MDC, VIC 3169 (Australia)
E-mail: kristina.konstas@csiro.au
matthew.hill@csiro.au
W. X. Lim, Dr. B. J. Cox, Prof. J. M. Hill
University of Adelaide, School of Mathematical Sciences
Adelaide SA 5005 (Australia)

[**] The authors acknowledge financial support from the CSIRO OCE science leader and postdoctoral fellowship schemes.

Supporting information for this article is available on the WWW under http://dx.doi.org/10.1002/anie.201201381.

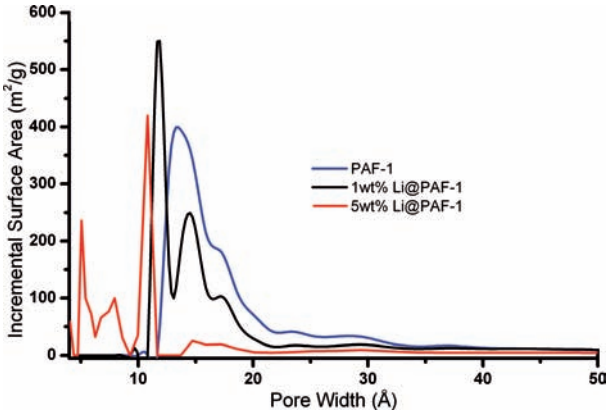

Figure 1. Pore-size distribution of PAF-1 (blue), 1%_Li@PAF-1 (black), and 5%_Li@PAF-1 (red) using results obtained from DFT fits to Ar adsorption isotherm data at 87 K.

within the pores in an organometallic state as Li^+ (Figure 2). Previously, microporous polymers have been lithiated under more facile conditions,[13a] resulting in an increase in gas storage capacities. Inspired by this approach, we adopted higher reaction temperatures, resulting in the lithiative reduction of PAF-1. The driving force for the reduced framework is the induced dynamic vacuum and elevated temperature conditions, forcing the removal of naphthalene and leaving behind reactive lithium ions. This allows for the unfavored reduction of the biphenyl system to proceed. ^{1}H NMR (Figure 2a) shows a clear upfield shift in the average range of resonances for the aromatic protons in 5%_Li@PAF-1 relative to native PAF-1, which is indicative

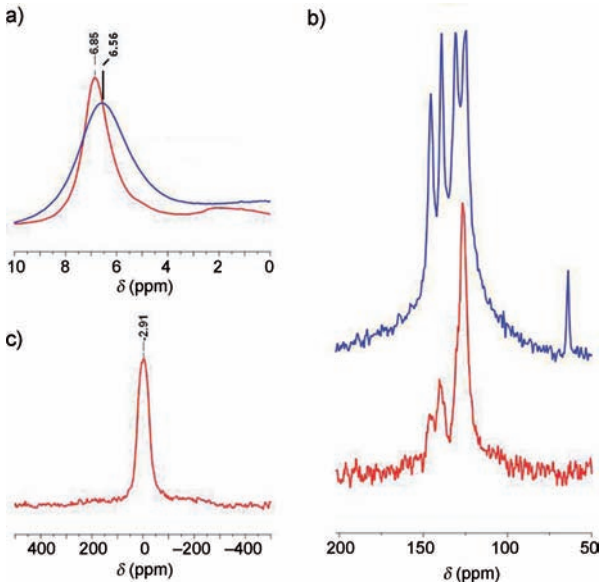

Figure 2. a) ^{1}H MAS NMR spectra of PAF-1 (red) and 5%_Li@PAF-1 (blue) with a spinning speed of 30 kHz and 7000 scans; b) ^{1}H–^{13}C CP/MAS NMR spectra of PAF-1 (blue) and 5% Li@PAF-1 (red) with a spinning speed of 12 kHz and 15000 scans; c) ^{6}Li MAS NMR spectrum of 5%_Li@PAF-1 with a spinning speed of 12 kHz and 5600 scans.

of the increase in local electron density owing to the reduced framework. The absence of naphthalene in both the ^{1}H and ^{13}C NMR spectra suggests complete activation for gas adsorption analysis. The ^{6}Li spectrum (Figure 2c) shows a peak at −2.91 ppm associated with organometallic Li^+ bound to aromatic carbons by cation–π and charge-transfer interactions, which balances the negative charge of the reduced framework.[20,24]

To further understand the performance of these materials, an atomistic simulation approach and a continuum modeling approach were used to explore the hydrogen storage capacity. Using the H_2-PAF potential energies (see the Supporting Information), H_2 uptakes at high pressure were calculated for PAF-1 and 2% and 5%_Li@PAF-1. The topographically integrated mathematical thermodynamic adsorption model (TIMTAM) results for total H_2 adsorption at 77 K and 50 bar (Figure 3) display a strong correlation with the original PAF-1 experimental data[17] and predict a significant increase in storage capacity upon lithiation.

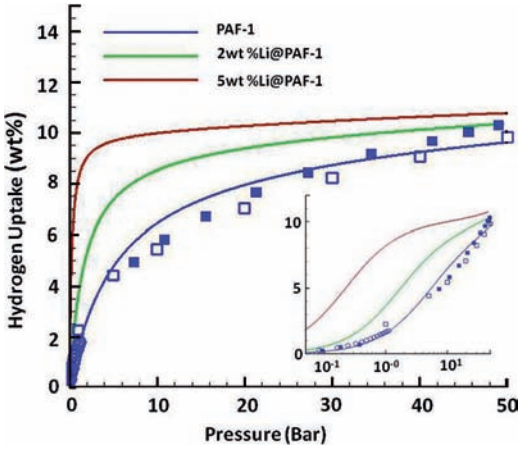

Figure 3. Computed high-pressure H_2 total uptake at 77 K using experimental[17] (■), atomistic simulation (□), and TIMTAM results (——). Inset: Log plot of the data from the original plot.

The TIMTAM approach can also be extended to investigate the optimal pore size for analogous PAF structures with lithium. Mapping the potential energy landscape gives a measure of the regions within the material in which gas can be stored in a densely adsorbed phase relative to compressed phases (Figure 4). Results indicate that the diphenyl subunits formed within PAF-1 are closest to delivering the optimal fractional free volume for adsorption within linear linker moieties. This simulation indicates that 30% of the space within 5%_Li@PAF-1 will contain hydrogen in the dense adsorbed phase, which explains the exceptional adsorption.

Gas adsorption isotherms were collected for Ar, CH_4, CO_2, and H_2 at either 77, 87, 273, and 298 K for 0, 1, 2, 5, and 10 wt% Li loading. Prior to measurement, samples were fully activated at 200°C under dynamic vacuum at 10^{-6} Torr for 24 h to remove any remaining naphthalene residues, and to fully complete the reductive lithiation.

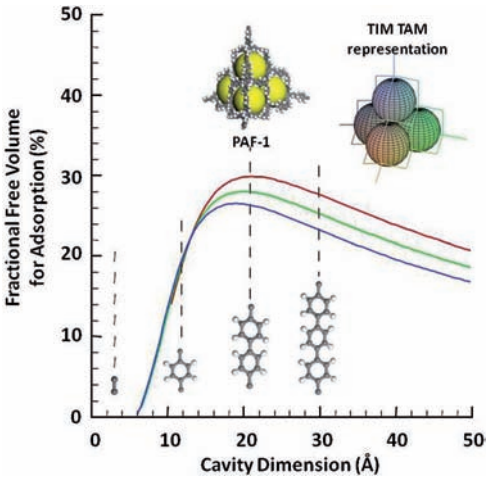

Figure 4. Fractional free volume for adsorption [%] calculated at 77 K, using the TIMTAM method with varying cavity dimensions (See the Supporting Information for details).

H_2 adsorption isotherms (Figure 5) collected at 77 K and 1.2 bar exhibit a storage capacity of 2.7 wt% for 5%_Li@PAF-1, which is amongst the highest reported for adsorbent-based storage materials for any lithiated doped material. Furthermore, H_2 adsorption experiments were performed on unactivated lithiated PAF-1 and lithium naphthalenide ($Li^+C_{10}H_8^{\bullet-}$) for verification of observed adsorption results (see the Supporting Information). We observed the 5%_Li@PAF-1 to have a 22% increase over the already large storage capacity found in PAF-1. In comparison, the recently reported MOF [Cu(Me-4py-trz-ia)] exhibits a low-pressure capacity of 3.07 wt%, with the maximum storage at higher pressures is somewhat diminished (4.1 wt%, 30 bar), which is possibly due to the comparatively lower surface area (see the Supporting Information).[25]

The high surface area of 5%_Li@PAF-1 (see the Supporting Information) means that while the adsorption capacity is exceptional at low pressures and amongst the highest reported, it can also perform high capacity storage for elevated pressure applications, with our simulations (Figure 3) revealing a total uptake capacity of 11 wt%. Enthalpy of adsorption measurements reveal the mechanism for the enhanced adsorption capacity, with all of the lithiated materials having a higher zero-coverage adsorption of enthalpy (Figure 5, inset), with the maximum of 9 kJ mol^{-1} close to the typical values reported in other lithiated adsorbents.[13a,20] 5%_Li@PAF-1 maintained a 2 kJ mol^{-1} enhancement over the native PAF, even at higher coverage. The reduced carbon framework in 5%_Li@PAF-1 will have a delocalized anionic charge and as such will be more attractive to hydrogen adsorption, similar to cationic point charges seen with unsaturated metal centers.[26]

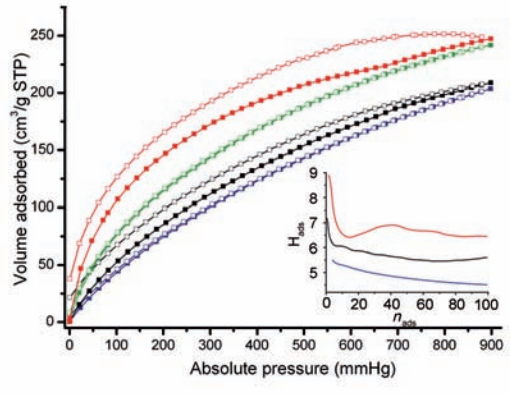

Figure 5. Experimental H_2 adsorption (■) and desorption (□) isotherms of PAF-1 (blue) and the lithiated PAFs (1%_Li@PAF-1, black; 2%_Li@PAF-1, green; 5%_Li@PAF-1, red) at 77 K. Inset: Heat of adsorption H_{ads} [kJ mol^{-1}] versus quantity adsorbed n_{ads} [cm^3 g^{-1} STP] of H_2 at 77 K and 87 K.

CO_2 uptakes at 273 K reveal a remarkable enhancement in CO_2 capture capacities upon reduction by lithiation (Figure 6). 5%_Li@PAF-1 has a CO_2 storage capacity of

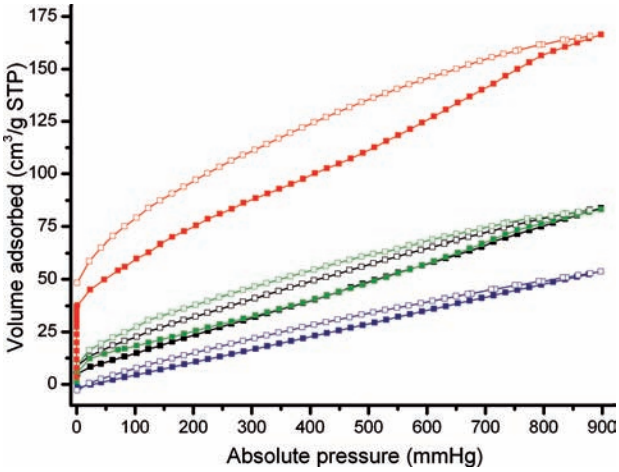

Figure 6. Experimental CO_2 adsorption (■) and desorption (□) isotherms of PAF-1 (blue) and the lithiated PAFs (1%_Li@PAF-1, black; 2%_Li@PAF-1, green; 5%_Li@PAF-1, red) at 273 K.

8.99 mmol g^{-1} at 273 K and 1.22 bar, which is amongst the highest reported for any material.[7] Similarly, as found with the H_2 uptakes, the relative high surface area of 5%_Li@PAF-1, means that saturation is not achieved until much higher pressures, enhancing the overall capacity of the material. This capacity largely comes about because of the exceptionally sharp uptake at low pressures, which is indicative of pseudo chemisorptive behavior between exposed Li^+ sites and CO_2. Indeed, isotherms recorded at 298 K have confirmed exceptionally strong adsorption enthalpies at zero coverage (see the Supporting Information). With higher Li loading levels, a diminished gas uptake capacity was observed owing to degradation of the sample and possibly the agglomeration of lithium ions. This is somewhat expected, as the maximum of one Li ion per phenyl ring is reached at a Li loading level of 8 wt%.

In conclusion, guided by computational simulation, a porous aromatic framework has been activated for gas adsorption by reductive lithiation. 5%_Li@PAF-1 demonstrates extremely large gas storage capacities for H_2, CO_2, and

CH_4 (11.03 mmol g^{-1}, 77 K, 1.22 bar; 8.99 mmol g^{-1}, 273 K, 1.22 bar; 1.30 mmol g^{-1}, 273 K, 1.22 bar, respectively), and these performances have been rationalized comprehensively by a range of characterization and simulation techniques after complete activation of the samples. The pore size of the activated framework 5%_Li@PAF-1 is found to be optimal for gas storage of H_2 at 77 K, and the exposed Li^+ sites exhibit pseudo chemisorptive behavior to CO_2 at 273 K, resulting in a 320% capacity enhancement over the native PAF-1.

Received: February 20, 2012
Revised: April 2, 2012
Published online: June 5, 2012

Keywords: adsorption · hydrogen · gas storage · lithiation · porous aromatic frameworks

[1] L. J. Murray, M. Dinca, J. R. Long, *Chem. Soc. Rev.* **2009**, *38*, 1294 – 1314.
[2] a) S. S. Han, W. Q. Deng, W. A. Goddard, *Angew. Chem.* **2007**, *119*, 6405 – 6408; *Angew. Chem. Int. Ed.* **2007**, *46*, 6289 – 6292; b) C. D. Wood, B. Tan, A. Trewin, H. J. Niu, D. Bradshaw, M. J. Rosseinsky, Y. Z. Khimyak, N. L. Campbell, R. Kirk, E. Stockel, A. I. Cooper, *Chem. Mater.* **2007**, *19*, 2034 – 2048; c) J. Y. Lee, C. D. Wood, D. Bradshaw, M. J. Rosseinsky, A. I. Cooper, *Chem. Commun.* **2006**, 2670 – 2672.
[3] S. Q. Ma, D. F. Sun, J. M. Simmons, C. D. Collier, D. Q. Yuan, H. C. Zhou, *J. Am. Chem. Soc.* **2008**, *130*, 1012 – 1016.
[4] a) T. Düren, L. Sarkisov, O. M. Yaghi, R. Q. Snurr, *Langmuir* **2004**, *20*, 2683 – 2689; b) C. D. Wood, B. Tan, A. Trewin, F. Su, M. J. Rosseinsky, D. Bradshaw, Y. Sun, L. Zhou, A. I. Cooper, *Adv. Mater.* **2008**, *20*, 1916 – 1921.
[5] M. Eddaoudi, J. Kim, N. Rosi, D. Vodak, J. Wachter, M. O'Keeffe, O. M. Yaghi, *Science* **2002**, *295*, 469 – 472.
[6] a) Z. Xiang, Z. Hu, D. Cao, W. Yang, J. Lu, B. Han, W. Wang, *Angew. Chem.* **2011**, *123*, 511 – 514; *Angew. Chem. Int. Ed.* **2011**, *50*, 491 – 494; b) P. L. Llewellyn, S. Bourrelly, C. Serre, Y. Filinchuk, G. Ferey, *Angew. Chem.* **2006**, *118*, 7915 – 7918; *Angew. Chem. Int. Ed.* **2006**, *45*, 7751 – 7754; c) D. M. D'Alessandro, T. McDonald, *Pure Appl. Chem.* **2010**, *83*, 57 – 66.
[7] D. M. D'Alessandro, B. Smit, J. R. Long, *Angew. Chem.* **2010**, *122*, 6194 – 6219; *Angew. Chem. Int. Ed.* **2010**, *49*, 6058 – 6082.
[8] S. R. Batten, S. M. Neville, D. R. Turner, *Coordination Polymers: Design, Analysis and Application*, Royal Society of Chemistry, Thomas Graham House, Science Park, Milton Road, Cambridge CB4 0WF, UK, **2008**.
[9] *Multi-Year Research, Development and Demonstration Plan—Planned Program Activities for 2003 – 2010: Technical Plan*; U.S. Department of Energy, http://www.eere.energy.gov/hydrogenandfuelcells/mypp/pdfs/storage.pdf; A. Celzard, V. Fierro, *Energy Fuels* **2005**, *19*, 573 – 583.
[10] K. Sumida, M. R. Hill, S. Horike, A. Dailly, J. R. Long, *J. Am. Chem. Soc.* **2009**, *131*, 15120 – 15121.
[11] A. W. Thornton, K. M. Nairn, J. M. Hill, A. J. Hill, M. R. Hill, *J. Am. Chem. Soc.* **2009**, *131*, 10662 – 10669.
[12] S. S. Kaye, A. Dailly, O. M. Yaghi, J. R. Long, *J. Am. Chem. Soc.* **2007**, *129*, 14176 – 14177.
[13] a) A. Li, R.-F. Lu, Y. Wang, X. Wang, K.-L. Han, W. Q. Deng, *Angew. Chem.* **2010**, *122*, 3402 – 3405; *Angew. Chem. Int. Ed.* **2010**, *49*, 3330 – 3333; b) Y. H. Jin, B. A. Voss, R. D. Noble, W. Zhang, *Angew. Chem.* **2010**, *122*, 6492 – 6495; *Angew. Chem. Int. Ed.* **2010**, *49*, 6348 – 6351; c) J. X. Jiang, A. Trewin, F. B. Su, C. D. Wood, H. J. Niu, J. T. A. Jones, Y. Z. Khimyak, A. I. Cooper, *Macromolecules* **2009**, *42*, 2658 – 2666; d) N. B. McKeown, P. M. Budd, *Macromolecules* **2010**, *43*, 5163 – 5176; e) E. Preis, C. Widling, U. Scherf, S. Patil, G. Brunklaus, J. Schmidt, A. Thomas, *Polym. Chem.* **2011**, *2*, 2186 – 2189; f) R. Short, M. Carta, C. G. Bezzu, D. Fritsch, B. M. Kariuki, N. B. McKeown, *Chem. Commun.* **2011**, *47*, 6822 – 6824.
[14] C. J. Doonan, D. J. Tranchemontagne, T. G. Glover, J. R. Hunt, O. M. Yaghi, *Nat. Chem.* **2010**, *2*, 235 – 238.
[15] a) J. X. Jiang, C. Wang, A. Laybourn, T. Hasell, R. Clowes, Y. Z. Khimyak, J. L. Xiao, S. J. Higgins, D. J. Adams, A. I. Cooper, *Angew. Chem.* **2011**, *123*, 1104 – 1107; *Angew. Chem. Int. Ed.* **2011**, *50*, 1072 – 1075; b) A. I. Cooper, *Angew. Chem.* **2011**, *123*, 1028 – 1030; *Angew. Chem. Int. Ed.* **2011**, *50*, 996 – 998; c) A. Trewin, A. I. Cooper, *Angew. Chem.* **2010**, *122*, 1575 – 1577; *Angew. Chem. Int. Ed.* **2010**, *49*, 1533 – 1535.
[16] T. Ben, H. Ren, S. Q. Ma, D. P. Cao, J. H. Lan, X. F. Jing, W. C. Wang, J. Xu, F. Deng, J. M. Simmons, S. L. Qiu, G. S. Zhu, *Angew. Chem.* **2009**, *121*, 9621 – 9624; *Angew. Chem. Int. Ed.* **2009**, *48*, 9457 – 9460.
[17] T. Ben, C. Pei, D. Zhang, J. Xu, F. Deng, X. Jing, S. Qiu, *Energy Environ. Sci.* **2011**, *4*, 3991 – 3999.
[18] D. Yuan, W. Lu, D. Zhao, H.-C. Zhou, *Adv. Mater.* **2011**, *23*, 3723 – 3725.
[19] S. K. Bhatia, A. L. Myers, *Langmuir* **2006**, *22*, 1688 – 1700.
[20] K. L. Mulfort, J. T. Hupp, *J. Am. Chem. Soc.* **2007**, *129*, 9604 – 9605.
[21] S. R. Batten, R. Robson, *Angew. Chem.* **1998**, *110*, 1558 – 1595; *Angew. Chem. Int. Ed.* **1998**, *37*, 1460 – 1494.
[22] J. L. C. Rowsell, O. M. Yaghi, *Angew. Chem.* **2005**, *117*, 4748 – 4758; *Angew. Chem. Int. Ed.* **2005**, *44*, 4670 – 4679.
[23] T. Hasell, C. D. Wood, R. Clowes, J. T. A. Jones, Y. Z. Khimyak, D. J. Adams, A. I. Cooper, *Chem. Mater.* **2010**, *22*, 557 – 564.
[24] I. Aprahamian, D. Eisenberg, R. E. Hoffman, T. Sternfeld, Y. Matsuo, E. A. Jackson, E. Nakamura, L. T. Scott, T. Sheradsky, M. Rabinovitz, *J. Am. Chem. Soc.* **2005**, *127*, 9581 – 9587.
[25] D. Lässig, J. Lincke, J. Moellmer, C. Reichenbach, A. Moeller, R. Gläser, G. Kalies, K. A. Cychosz, M. Thommes, R. Staudt, H. Krautscheid, *Angew. Chem.* **2011**, *123*, 10528 – 10532; *Angew. Chem. Int. Ed.* **2011**, *50*, 10344 – 10348.
[26] M. Dincă, J. R. Long, *Angew. Chem.* **2008**, *120*, 6870 – 6884; *Angew. Chem. Int. Ed.* **2008**, *47*, 6766 – 6779.